International Journal of Aviation, Aeronautics, and Aerospace

Volume 10 | Issue 3 Article 4

2023

Accuracy Assessment of the eBee Using RTK and PPK Corrections Methods as a Function of Distance to a GNSS Base Station

Joseph Cerreta
Embry-Riddle Aeronautical University, cerretaj@erau.edu
David Thirtyacre
Embry-Riddle Aeronautical University, thirtyad@erau.edu
Peter Miller
Warren County Community College, pmiller2@warren.edu
Scott S. Burgess
Embry-Riddle Aeronautical University, burgesco@erau.edu
William J. Austin
Warren County Community College, will@warren.edu

Scholarly Commons Citation

Cerreta, J., Thirtyacre, D., Miller, P., Burgess, S. S., & Austin, W. J. (2023). Accuracy Assessment of the eBee Using RTK and PPK Corrections Methods as a Function of Distance to a GNSS Base Station. *International Journal of Aviation, Aeronautics, and Aerospace, 10*(3). DOI: https://doi.org/10.58940/2374-6793.1819

The use of Unmanned Aircraft Systems (UAS) to collect data for photogrammetry products, such an orthomosaic and Digital Elevation Model (DEM) has grown significantly in recent years (Chaudhry et al., 2020; Room et al., 2019). One of the key advantages of using UAS for surveying is the speed at which data can be collected. UAS can cover large areas quickly, making them ideal for surveying applications that require fast results. UAS can also be flown in areas that are difficult or dangerous to access, such as steep terrain, coastal cliffs, or areas affected by natural disasters (Žabota et al., 2021). UAS can capture data from a variety of altitudes, providing a unique perspective that is not possible with traditional surveying techniques.

The accuracy of a photogrammetric model can depend on image overlap, quality, and georeferencing. The distance from a reference base station can affect the accuracy of the results (Baybura et al., 2019). Positioning corrections data relies on precise timing measurements of satellite signals. The signals travel through the Earth's atmosphere, which introduces errors due to ionospheric and tropospheric delays (Gou et. al., 2011). Additionally, Gomez et. al. (2021) suggested the distribution of ground control points (GCPs) can affect accuracy when using non-precision GNSS positioning of the aircraft or images. A GCP is a target placed on the ground (see Figure 1), within a mapping area of interest, with a known high-precision location assigned to it. The high-precision location coordinates are often determined by using traditional Global Navigation Satellite System (GNSS) survey methods. The GCPs are visible to the UAS overhead during the data collection process. Traditionally, each GCP is marked in photogrammetry software to correct the model to the known locations. In this research all GCPs were used as Check Points (CPs) to validate the accuracy of the photogrammetry model to the measured CP location with a rover GNSS receiver instead. CPs are not considered by the photogrammetry software to correct any errors in the model, only to measure its accuracy.

Figure 1

Check Points Used in Data Collection

Note. CP1 (left) and CP3 (right) from flying site #3.

Room et al. (2019) suggested a direct correlation to the number of GCPs in a mapping area of interest and global position accuracy. Villanueva and Blanco (2019) showed a positive relationship between the number of GCPs and global accuracy in a photogrammetry product, whereas the global accuracy was higher when greater numbers of GCPs were used. GCP emplacement requires additional time to install the targets and measure their location with traditional GNSS survey equipment (Žabota et. al., 2021). Štroner, et. al. (2020) suggested using

UAS equipped with a high-precision GNSS would not require GCPs at all to correct the accuracy of the photogrammetry models. Famiglietti et.al. (2021) also suggested that integrating the high-precision positioning georeferencing data in each image, known as geotagging, could produce the same level of accuracy as if using GCPs, eliminating the need for GCPs altogether, which is particularly beneficial in areas of large topographical changes, such as steep terrain.

One such UAS that has gained popularity is the senseFly eBee X (AgEagle, 2023a). The eBee X is a fixed-wing drone that is designed for high-precision mapping and surveying. One of the key features of the eBee X is its GNSS receiver capability. The GNSS system includes both GPS and GLONASS receivers, which enable the drone to receive signals from multiple satellite constellations simultaneously. According to the manufacturer, the eBee X was designed to achieve global horizontal position accuracy of up to 1.5 cm, and vertical accuracy of up to 3 cm (AgEagle, 2023c). This level of accuracy is achieved using Real Time Kinematic or Post-Processed Kinematic methods. The eBee X can use both positioning methods, depending on the requirements of the specific application.

The global accuracy of a photogrammetry model can be assessed using root-mean-square error (RMSE) and standard deviation (SD) calculations between the model and its CPs (Štroner, et.al., 2020; Villanueva and Blanco, 2019). The RMSE is a measure of the accuracy of a photogrammetry model by measuring the difference between the predicted and observed values, such as its photogrammetric-calculated position and traditionally surveyed position of a CP. Smaller RMSE and SD values indicate higher accuracy and precision of the photogrammetry model.

Advantages and Disadvantages Between RTK and PPK Positioning

The most significant advantage of RTK over PPK is the ability to obtain real-time positioning results (Tae-Suk Bae, 2019). RTK provides immediate, real-time corrections to the rover's position based on the data received from the base station. This real-time capability allows for instant corrections and ensures that the eBee X’s position is continuously updated for high accuracy positioning. In contrast, PPK requires the collected data to be post-processed after the flights are completed, which means there is a delay between data collection and obtaining the final position results. Depending on the source of the base station corrections, the delay may be up to 24 hours for some CORS base stations (UNAVCO, 2023a). RTK's real-time capability is particularly valuable in applications that require immediate positioning information or in scenarios where dynamic or time-sensitive measurements are involved.

While RTK has several advantages over PPK, it also has some disadvantages. One of the significant disadvantages of RTK is its limited range (Room et al, 2019; Štroner et al., 2020). RTK positioning is generally limited to several kilometers from the base station. Beyond this range, the corrections transmitted from the base station may not be sufficient to compensate for atmospheric errors and other factors affecting positioning accuracy. In contrast, PPK can be used over much larger distances, as it is not constrained by the need for real-time corrections.

RTK requires a continuous internet connection between the base station and the eBee X’s ground station using the eMotion flight control software for accurate positioning. However, signal interference can occur from obstructions such as buildings, trees, or terrain, reducing the quality of the measurements and the accuracy of the results. This can be particularly problematic in urban or forested environments where signal blockage and multipath interference are common (Tomaštík et al., 2019). In contrast, PPK can collect GNSS data from the eBee X and base station independently, while not requiring a continuous internet connection, making it more robust to signal blockage and interference.

An advantage of PPK is the need for less infrastructure compared to RTK. RTK requires a base station to be set up in the field, over a known location, to transmit correction data to the rover. This can add to the cost of having a dedicated base station and logistical challenges of emplacing the RTK base station on a known point for the greatest level of positional accuracy. In contrast, PPK only requires a GNSS receiver on the eBee X and a virtual base station, such as a publically-accessible CORS station (UNAVCO, 2023a), making it a more straightforward and cost-effective solution.

Baseline Distance Effect on GNSS Accuracy

The distance from a GNSS base station can affect the accuracy of the results obtained from RTK or PPK methods (Baybura et. al., 2019). RTK and PPK positioning relies on precise timing measurements of satellite signals. The signals travel through the Earth's atmosphere, which introduces errors caused by ionospheric and tropospheric delays (Gou et al., 2011). These errors are generally spatially correlated and affect both the base station and the rover. The further the eBee X is from the base station, the greater the GNSS accuracy can decrease. The focus of this research is to investigate the influence of the distance from the base station to the eBee X with RTK and PPK corrections and the observed accuracy.

Other factors that can affect the accuracy of the positioning data, which were not investigated in this research, included terrain, number of GNSS satellites, signal interference, and the accuracy of the base station itself (Zimbelman et al., 2019). The terrain can affect GNSS accuracy. Uneven terrain can cause reflections of GNSS signals, resulting in multipath errors. Multipath errors occur when the signal from the satellite bounces off nearby surfaces, such as trees, buildings, or other structures, before reaching the drone (Chen et al., 2022). These reflections can cause errors in the GNSS measurements, which can affect the accuracy of the final map or survey. The accuracy of the base station data providing corrections to the eBee X can also affect GNSS accuracy. If the base station data is not accurate, then the GNSS system may not be able to provide accurate positioning data. The base station should be emplaced over a known point, which is a previously surveyed, traditionally marked location on the ground.

Methods

The aim of this research was to examine the eBee X and its global GNSS accuracy by comparing the RTK and PPK methods at different base station distances in photogrammetry models. Three factors were investigated, these were, 1) RTK and PPK methods, 2) local GNSS receiver via caster and NTRIP corrections sources, and 3) base station distances between 2.4 km and 42.0 km. A Reach RS2 local and CORS GNSS base stations were used. The data consisted of images collected by the eBee X, which were imported into Pix4Dmapper (Pix4d, 2023) to create photogrammetry models of each flight. The RMSE values of eight CPs from three flying sites in the photogrammetry models were compared.

Study Area

As depicted in Figure 2, the study area consisted of three locations in Southwest Arizona in the United States between Yuma and Wellton, Arizona. Three areas were selected based on their distance from either a Reach RS2 local base station or CORS station. The areas were also selected based on their accessibility and ability to fly the eBee X. Accessibility was determined by access via public roads and the flying site. The ability for the eBee X to fly was determined by selecting areas within uncontrolled airspace.

Figure 2
Study Area Map

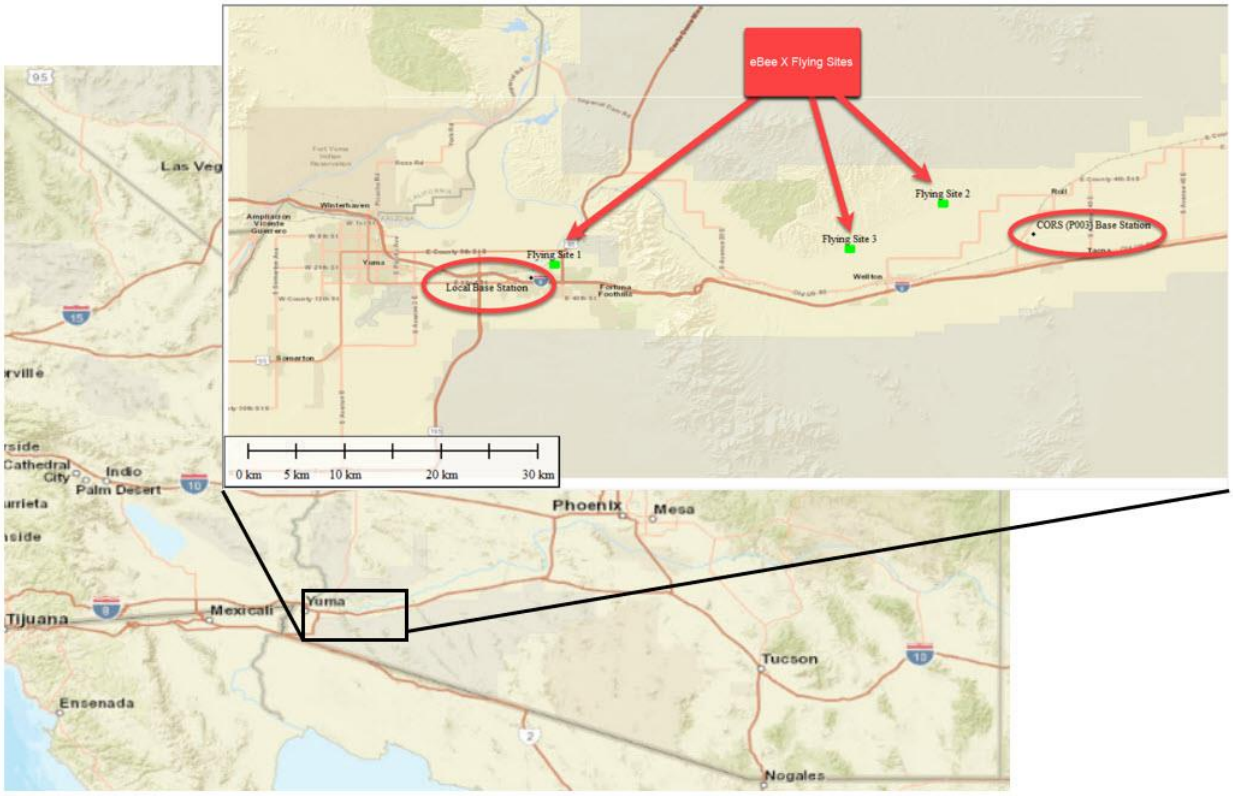

Note. Southwest US depicting the study area location with two GNSS base stations and three flying sites. [Map] Global Mapper v22.1.

Base Station Information

Two base stations were used. A local base station consisted of an Emlid Reach RS2 (Emlid, 2023a) located in Yuma, Arizona. The Reach RS2 is a multi-band receiver that works as a base for RTK and PPK global positioning corrections. The RS2 was set up on a known location via tripod with a 1.83 m antenna reference point. The known location was established using the Online Positioning User Service (OPUS) provided by the U.S. National Geodetic Survey (NGS) (NGS, 2023), the RS2 collected base station observations in the Receiver Independent Exchange Format (RINEX). Six hours of static position observations were collected then uploaded to the OPUS server to process the data. An OPUS solution was processed from the observations using three CORS reference stations (P506, GMPK, and P003) consisting of $RMSE_X$ = 0.009m, $RMSE_Y$ = 0.007m, and $RMSE_Z$ = 0.011m for the RS2 base station position. The OPUS solution report provided the base coordinates in the International Terrestrial Reference System (ITRF) 2014 coordinates, which were transformed into the WGS84 coordinate system in meters and an ellipsoidal height. The local base station was accessed via Emlid Caster (Emlid, 2023b) to the eMotion flight control software to enable real-time corrections to the eBee X during the RTK-local base enabled flights. Also, RINEX version 2.11 files were retrieved from the RS2 for the PPK processing.

The UNAVCO P003 CORS base station was selected as the second station (UNAVCO, 2023b). P003 was located in Wellton, Arizona. P003 provided RTK broadcasts for centimeter-level corrections throughout the RTK-P003 enabled flights. P003 also recorded RINEX observations,

which were used in the post processing of the PPK methods. The RMSE was averaged for P003 for all flight days as $RMSE_X$ = 0.002m, $RMSE_Y$ = 0.002m, and $RMSE_Z$ = 0.007m. P003 was accessed via an NTRIP service to the eMotion flight control software to enable real-time corrections to the eBee X during the RTK-P003 flights.

CP Data Collection

A second Emlid Reach RS2 collected CP location data for each of the eight CPs at each of the three flying sites. The RS2 used the RTK method and connected either to the local base RS2 or the P003 CORS base station, whichever was closer for each flying site, to obtain high precision location data to mark each CP. As shown in Figure 1 above, the RS2 rover was emplaced over the center of each CP using a bipod, an antenna reference point of 1.83 m, and leveled via bubble level. Three 20-second measurements were taken for each of the eight CPs at each of the three flying sights. The three measurements were then averaged to obtain the final position of each CP in the WGS84 coordinate system with an ellipsoid height. A comma separated values file was generated for the CPs at each of the three flying sites. The RMSE of the second rover RS2 for each CP axis for each flying location was shown in Table 1.

Table 1

CP RMSE Values for Each Flying Site

Flying Site	RMSE X	RMSE Y	RMSE Z
1	0.010	0.010	0.011
2	0.010	0.010	0.017
3	0.010	0.011	0.019

Note. The units are in meters. Measurements reflect the relative RMSE between the second rover Reach RS2 and the base station position.

Flying Sites and GCP Distribution

Each of the three flying sites had the same dimensions as the area of interest. The dimensions were 570 m along an East-West orientation by 388 m along a North-South orientation. The area was 0.22 km^2. As depicted in Figure 3, CPs were distributed in a bow-tie configuration for each of the three flying sites.

Figure 3

Bow-Tie Distribution of CPs for Each Flying Site

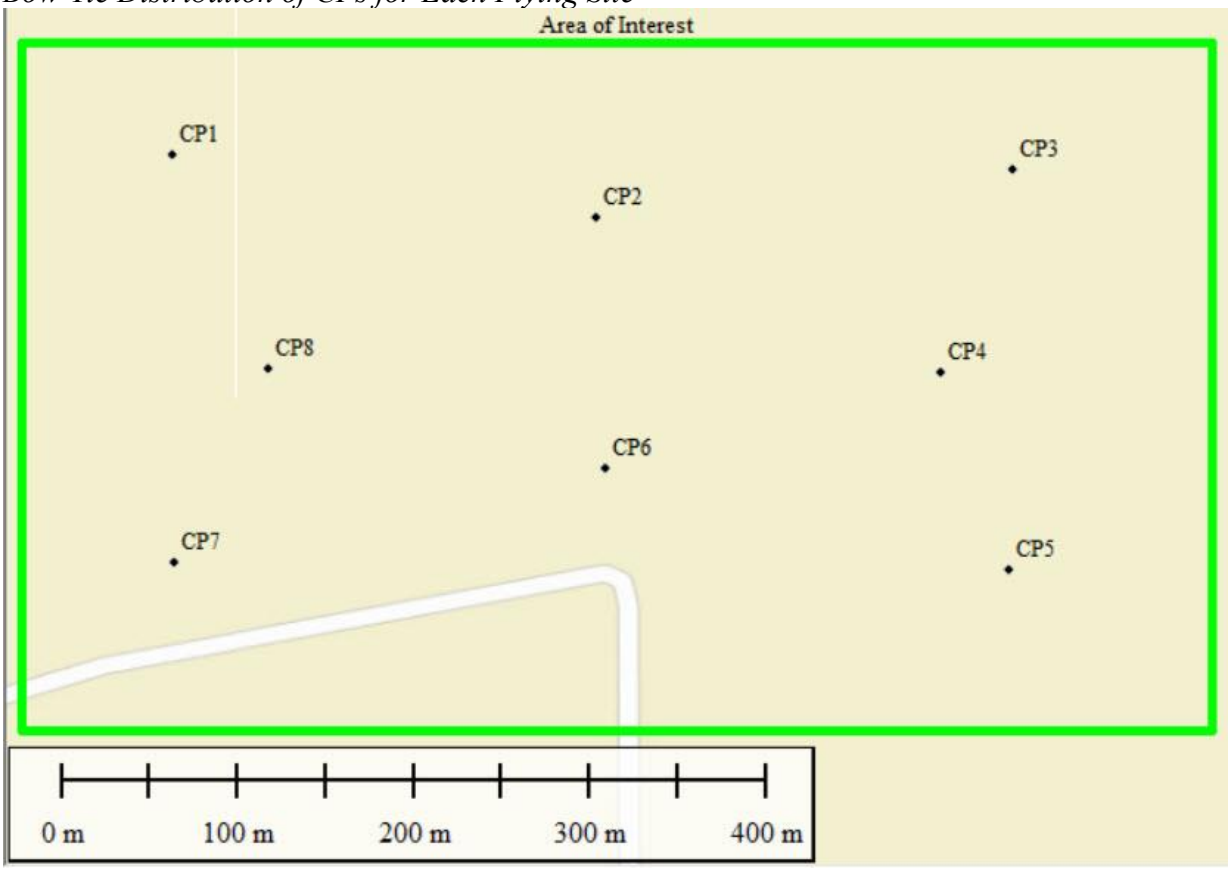

Note. CP locations distributed in a bow-tie configuration within the area of interest. [Map] Global Mapper v22.1.

Data Collection with the eBee X

An eBee X was flown between Mar 16, 2023, and April 21, 2023, at three different flying sites to obtain GNSS corrections data from two base stations at six different distances. Table 2 depicts the flight dates and sites. Each flying site consisted of the same size area of interest, which was a KML file imported into the eMotion flight control software. The eBee X flew a single grid pattern in an East-West orientation, along the longest side of the area of interest. Figure 3 depicts the KML file shown as a green rectangle with the eBee X's flight lines overlaid on top of the area of interest.

Table 2

eBee X Flights by Date, Site Number, and Base Station Distance

Flight Number	Date	Flying Site	Local Base Station Distance (km)	CORS Base Station Distance (km)
1, 2, 3, 4	16-Mar-23	Site 1	2.4	42.0
5, 6, 7, 8	29-Mar-23	Site 1	2.4	42.0
9, 10, 11, 12, 13	31-Mar-23	Site 1	2.4	42.0
14, 15, 16, 17, 18, 19, 20, 21	17-Apr-23	Site 2	36.5	8.4
22	19-Apr-23	Site 2	36.5	8.4
23	19-Apr-23	Site 3	27.8	16.2
24, 25, 26, 27	20-Apr-23	Site 3	27.8	16.2
28, 29, 30, 31, 32, 33	21-Apr-23	Site 3	27.8	16.2

Note. Flight numbers consist of either RTK or PPK corrections. Underlined flights indicate when RTK methods were used.

Figure 4

eMotion Screenshot Showing the Flight Planning for Flying Site #1

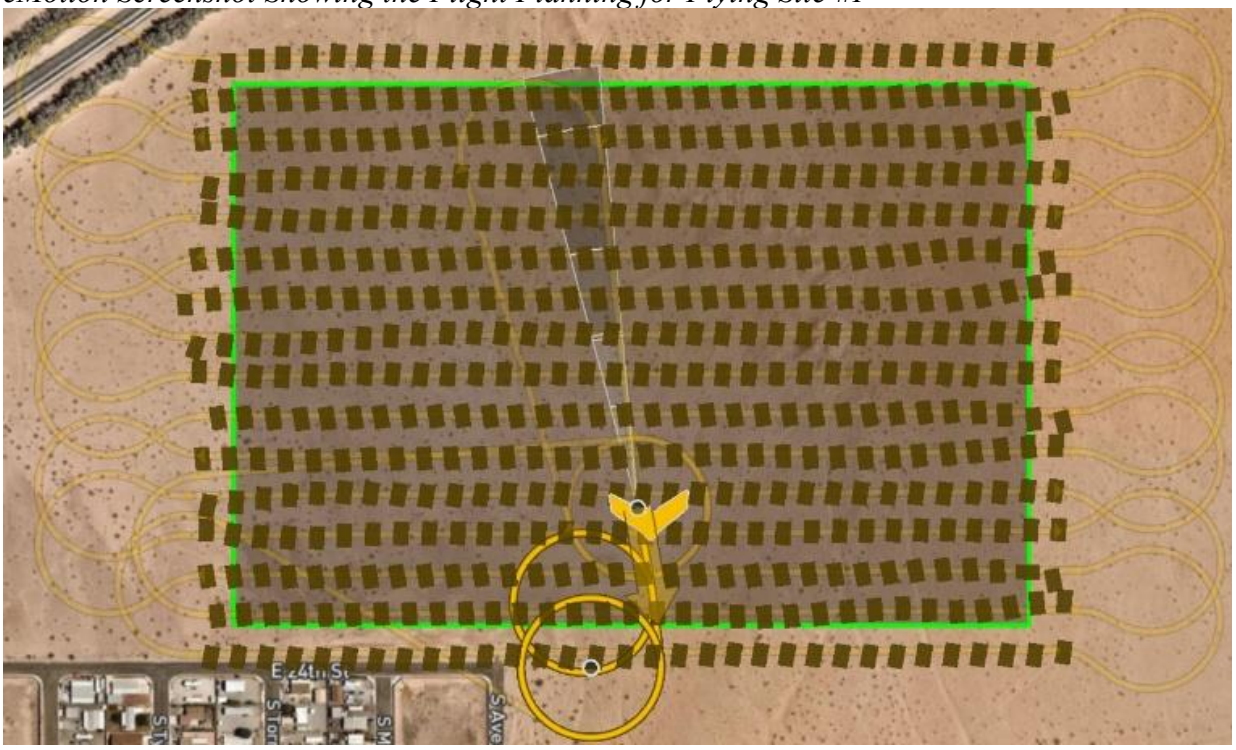

Note. Each image collected was shown as a camera footprint in the eMotion flight control software. [Software] eMotion.

Each of the 33 flights took approximately 22 minutes and consisted of an average of 514 images. The flying height was approximately 92 m, yielding a ground sample distance (GSD) of 0.02 m per pixel. According to Pix4D (2019), the expected accuracy results should be between 1-2 times the GSD horizontally and 2-3 times the GSD vertically. Based on the Pix4D expected accuracy results and the GSD flown, the expected $RMSE_{XYZ}$ accuracy for this research is 0.09 m (rounded up). Each flight was conducted on a single battery. Flight 31 was conducted in two parts because the eMotion flight control software lost the internet connection, resulting in the RTK

corrections stopping at approximately halfway through the flight. A second flight was continued from the last point to complete the data collection for Flight 31 in RTK mode. The loss of internet access and subsequent RTK corrections highlighted a benefit of using PPK corrections, whereas a continuous internet connection was not required.

Post-Processing of Data

After each flight, the eBee X log file, images, and RINEX files (for PPK-enabled flights) were retrieved. The eMotion software enabled an eight-step process to incorporate the RTK or process the PPK corrections by revising the geoinformation in the EXIF data for each image. Flights performed using RTK corrections were already geotagged with the corrected position data; however, re-tagging the EXIF data for each image and a geoinformation text file were still processed in the eMotion software to maintain a consistent post-processing process, regardless of using the RTK or PPK corrections method. Upon completion of the eight post-flight processing steps, image geotags, geoinformation text file were written to import the data into the photogrammetry software.

Pix4Dmapper (Pix4D, 2023) version 4.7.4 aligned each image dataset using the 3D Maps processing options template. The default options setting for the template maintained consistent processing between all 33 datasets. An Excel file containing the average position for each of the eight CPs, for each flying site, using the EPSG 4326 coordinate system and ellipsoid height in meters was imported into each of the 33 datasets. Processing step 1 was completed in Pix4Dmapper to calibrate each dataset of images, perform the aerial triangulation, and the bundle block adjustment. A single operator marked each CP with every image containing the CP in Pix4Dmapper. A single operator was used to maintain consistency of marking the CP locations. After marking each CP with every possible image available in each dataset, the photogrammetry project was reoptimized to determine the accuracy of the GNSS-corrected geoinformation, regardless if the RTK or PPK method was used. A quality report was generated to calculate the eight CP values of $RMSE_X$, $RMSE_Y$, and $RMSE_Z$ in Pix4Dmapper for each dataset. $RMSE_{XYZ}$ was calculated using equations 1 to determine the total accuracy of each dataset.

(1)
$$RMSE_{XYZ} = \sqrt{\frac{1}{n}\sum_{i=1}^{n}\left(\Delta\mathrm{RMSE}_{X_i}^{2} + \Delta\mathrm{RMSE}_{Y_i}^{2} + \Delta\mathrm{RMSE}_{Z_i}^{2}\right)}$$

Results

Thirty-three datasets were collected to determine if three factors affected the accuracy of each dataset for the eBee X. The factors compared were, 1) between RTK and PPK methods, 2) local Reach RS2 GNSS receiver via caster between P003 CORS receiver via NTRIP service, and 3) base station distances between 2.4 km and 42.0 km. A one-way ANOVA compared the $RMSE_{XYZ}$ from each dataset by each of the three factors.

A one-way ANOVA test examined differences in $RMSE_{XYZ}$ between RTK and PPK methods as well as between using a local Reach RS2 GNSS receiver via caster and NTRIP service. As depicted in Figure 5a, the ANOVA tests yielded a main effect for the observations by method, $F(1, 33) = 0.08$, $p = 0.778$, such that the mean was not significantly different for the RTK method ($M = 0.13$, $SD = 0.07$) compared to the PPK method ($M = 0.12$, $SD = 0.08$). As depicted in Figure 5b, the ANOVA tests yielded a main effect between using a local Reach RS2 GNSS receiver via caster and NTRIP service, $F(1, 33) = 0.90$, $p = 0.351$, indicating that the mean was not significantly different for the local Reach RS2 GNSS receiver via caster method ($M = 0.11$, $SD = 0.07$) compared

to the P003 CORS NTRIP service (M = 0.13, SD =0.09).These data suggest there was no significant difference in $RMSE_{XYZ}$ accuracy between RTK and PPK GNSS corrections methods or between a local Reach RS2 GNSS receiver via caster and P003 NTRIP service for the eBee X.

Figure 5 (a and b)

Boxplots of $RMSE_{XYZ}$ by RTK or PPK GNSS Corrections Methods and by Local Reach RS2 via Caster and P003 NTRIP GNSS Corrections Methods

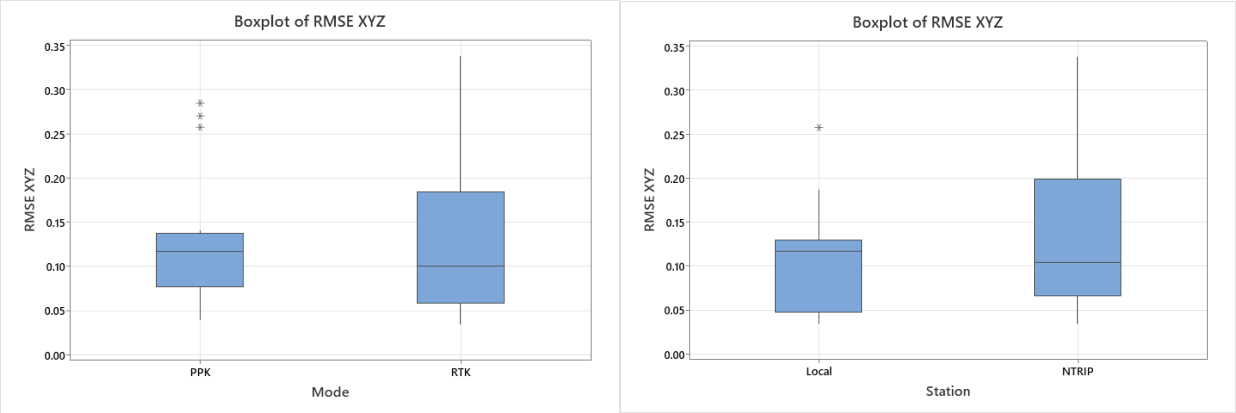

Note. Figure 5a, left, depicts differences between RTK and PPK methods. Figure 5b, right, depicts differences between the local Reach RS2 and P003 NTRIP service. Units in meters. The mean is represented by the line in the box. The interquartile range box represents the middle 50% of the data and shows the distance between the first and third quartiles (Q3-Q1). The whiskers represent the ranges for the bottom 25% and the top 25% of the data values, excluding outliers. Astricts denote outliers. [Software] Minitab 2023.

A one-way ANOVA test examined differences in $RMSE_{XYZ}$ between base station distances between 2.4 km and 42.0 km. Table 3 depicts the descriptive statistics for the differences. As depicted in Figure 7, the ANOVA tests yielded a main effect for the observations by method, $F(5, 33) = 11.99$, $p = 0.000$, such that the mean had a significant difference between base station differences. These data suggest there was a significant difference in $RMSE_{XYZ}$ accuracy based on the distance from the GNSS receiver base station providing corrections for the eBee X.

Table 3

Descriptive Statistics of Base Stations Distances and $RMSE_{XYZ}$ values

Distance from Base Station (km)	*N*	*M*	*SD*
2.4	6	0.06	0.04
8.4	4	0.06	0.02
16.2	7	0.09	0.02
27.8	4	0.14	0.03
36.5	5	0.15	0.06
42.0	7	0.23	0.07

Note. The distance from the base stations was in km. $RMSE_{XYZ}$ *M* and *SD* values in meters. According to Pix4D, the expected $RMSE_{XYZ}$ values were 0.09m or less.

Figure 7

Boxplot of $RMSE_{XYZ}$ by Base Station Distances

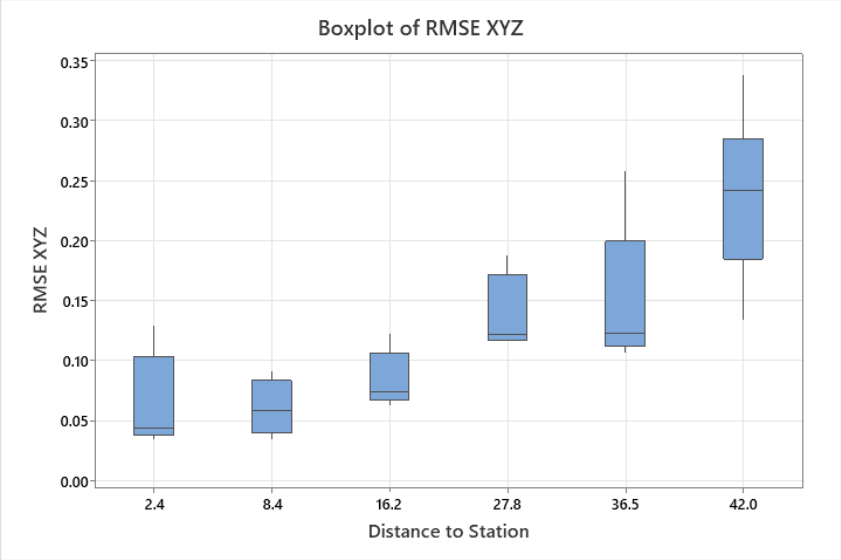

Note. $RMSE_{XYZ}$ units in meters. Distance to station units in km. [Software] Minitab 2023.

Conclusion

The eBee X equipped with RTK or PPK GNSS corrections enables direct georeferencing of a photogrammetric model without the need to use GCPs. This study has demonstrated that the eBee X with either RTK or PPK corrections information is capable of high accuracy measurements. An accuracy with an $RMSE_{XYZ}$ of less than 0.09 m was achieved in the CP observations when the GNSS base station was less than 16.2 km from the eBee X during the RTK or PPK GNSS position corrected flights.

These data support Baybura, et. al., (2019), which argues that RMSE accuracy was correlated to the distance from the station. The results have shown how using base station distances of less than 16.2 km considerably improves model accuracy, placing them in within the Pix4D claim of 1-2 times the GSD horizontally and 2-3 times the GSD vertically. It is recommended that eBee X users seeking to obtain the highest level of accuracy in their photogrammetry models use RTK or PPK corrections with a base station distance of less than 16.2 km.

References

AgEagle. (2023a). *eBee X UAS*. https://ageagle.com/drones/ebee-x/

AgEagle. (2023b). *eMotion flight control software*. https://ageagle.com/drone-software/emotion/

AgEagle. (2023c). *eBee X – Lightweight regulatory compliant mapping drone*. https://ageagle.com/drones/ebee-x/

Baybura, T., Tiryakioglu, I., Uğur, M. A., Solak, H., I., & Şafak, S. (2019). Examining the accuracy of network RTK and long base RTK methods with repetitive measurements. *Journal of Sensors 2019(4),* 1-12. 10.1155/2019/3572605

Chaudhry, M. H., Ahmad, A., & Gulzar, Q. (2020). A comparative study of modern UAV platform for topographic mapping. IOP Conference Series. *Earth and Environmental Science, 540(1),* 12019. https://doi.org/10.1088/1755-1315/540/1/012019

Chen, D., Ye, S., Xia, F., Cheng, X., Zhang, H., & Jiang, W. (2022). A multipath mitigation method in long-range RTK for deformation monitoring. *GPS Solutions, 26*(3). https://doi.org/10.1007/s10291-022-01281-9

Emlid. (2023a). *Reach RS2 multi-band RTK GNSS receiver*. http://files.emlid.com/docs/Datasheet%20RS2%20ENG%20web.pdf

Emlid. (2023b). *Emlid caster*. https://emlid.com/ntrip-caster/

Famiglietti, N. A., Cecere, G., Grasso, C., Memmolo, A., & Vicari, A. (2021). A test on the potential of a low cost unmanned aerial vehicle RTK/PPK solution for precision positioning. *Sensors, 21*(11), 3882. https://doi.org/10.3390/s21113882

Gomes Pessoa, G., Caceres Carrilho, A., Takahashi Miyoshi, G., Amorim, A., & Galo, M. (2021). Assessment of UAV-based digital surface model and the effects of quantity and distribution of ground control points. *International Journal of Remote Sensing, 42(1)*, 65–83. https://doi.org/10.1080/01431161.2020.1800122

Guo, H., He, H., Li, J., & Wang, A. (2011). Estimation and mitigation of the main errors for centimetre-level compass RTK solutions over medium-long baselines. *Journal of Navigation, 64*(S1), S113–S126. https://doi.org/10.1017/S0373463311000324

NGS. (2023). *Online positioning user service*. https://www.ngs.noaa.gov/OPUS/index.jsp

NOAA. (2023). *The NOAA CORS network (NCN).* https://geodesy.noaa.gov/CORS/

Pix4D. (2019). *What is accuracy in an aerial mapping project?* https://www.pix4d.com/blog/accuracy-aerial-mapping/

Pix4D. (2023). *Pix4Dmapper*. https://www.pix4d.com/product/pix4dmapper-photogrammetry-software/

Room, M. H. M., Ahmad, A., & Rosly, M. A. (2019). Assessment of different unmanned aerial vehicle system for production of photogrammetry products. *International Archives of the Photogrammetry, Remote Sensing and Spatial Information Sciences.*, XLII-4/W16, 549–554. https://doi.org/10.5194/isprs-archives-XLII-4-W16-549-2019

Štroner, M., Urban, R., Reindl, T., Seidl, J., & Brouček, J. (2020). Evaluation of the georeferencing accuracy of a photogrammetric model using a quadrocopter with onboard GNSS RTK. *Sensors, 20*(8), 2318. https://doi.org/10.3390/s20082318

Tae-Suk Bae. (2019). Network-based RTK performance for drone navigation. *E3S Web of Conferences, 94*, 01006. https://doi.org/10.1051/e3sconf/20199401006

Tomaštík, J., Mokroš, M., Surový, P., Grznárová, A., & Merganič, J. (2019). UAV RTK/PPK method—An optimal solution for mapping inaccessible forested areas? Remote *Sensing, 11*(6), 721. https://doi.org/10.3390/rs11060721

UNAVCO. (2023a). *Instrumentation networks: All networks and stations*. https://www.unavco.org/instrumentation/networks/networks.html

UNAVCO. (2023b). *P003 CORS reference station information*. https://www.unavco.org/instrumentation/networks/status/nota/overview/P003

Villanueva, J. K. S., & Blanco, A. C. (2019). Optimization of ground control point (GCP) configuration for unmanned aerial vehicle (UAV) surveying using structure from motion (SFM). *International Archives of the Photogrammetry, Remote Sensing and Spatial Information Sciences*, XLII-4/W12, 167–174. https://doi.org/10.5194/isprs-archives-XLII-4-W12-167-2019

Žabota, B., & Kobal, M. (2021). Accuracy assessment of UAV-photogrammetric-derived products using PPK and GCPs in challenging terrains: In search of optimized rockfall mapping. *Remote Sensing, 13*(19), 3812. https://doi.org/10.3390/rs13193812

Zimbelman, E. G., & Keefe, R. F. (2018). Real-time positioning in logging: Effects of forest stand characteristics, topography, and line-of-sight obstructions on GNSS-RF transponder accuracy and radio signal propagation. *PloS One, 13*(1), e0191017–e0191017. https://doi.org/10.1371/journal.pone.0191017